Hindawi
Advances in Materials Science and Engineering
Volume 2022, Article ID 5955725, 18 pages
https://doi.org/10.1155/2022/5955725

Research Article

Research on Optimization of Injection Molding Process Parameters of Automobile Plastic Front-End Frame

Kai Yang, Lingfeng Tang, and Peng Wu

School of Mechanical Engineering, Anhui Polytechnic University, Yangkai, Anhui 241000, China

Correspondence should be addressed to Kai Yang; 2210120108@stu.ahpu.edu.cn

Received 2 April 2022; Revised 2 October 2022; Accepted 11 October 2022; Published 20 October 2022

Academic Editor: Hao Yi

The main objective of the present article is to obtain the optimum technological parameters of the automobile plastic front-end frame. Moldflow software was used to simulate the injection molding of the automobile plastic front-end frame bracket in this study. The uniformity experiment was designed and completed. Five injection molding process parameters, including mold temperature, melt temperature, packing pressure, injection time, and packing time, were selected as experimental factors. Volume shrinkage and warpage amount were selected as quality evaluation indexes. Statistical Product Service Solutions (SPSS) software was used to perform linear regression analysis on the test results, respectively, and the linear regression equation corresponding to the two evaluation indexes was obtained. Then, regression equation analysis was carried out to obtain the optimal process parameter combination of the volume shrinkage and the warpage amount. A back propagation (BP) neural network model with input as a process parameter and output as an evaluation index is established by MATLAB and optimized by a genetic algorithm (GA). Finally, the optimized neural network model was used to predict the combination of process parameters with the minimum volume shrinkage and warpage amount. Based on the performed simulations, the minimum volume shrinkage and the minimum amount of warping in the optimal design were 13% and 0.7062 mm, respectively. The corresponding combination of process parameters was the mold temperature of 75.5°C, the melt temperature of 285.32°C, the packing pressure of 42.32 MPa, the injection time of 3.45 s, and the packing time of 60 s. According to the optimal process parameters, the volume shrinkage and warpage amount of the automobile plastic front-end frame have reached the optimal state at the same time, which improves the quality of injection molding and reduces production and processing costs. It has a certain guiding significance.

1. Introduction

With the rapid development of the plastic industry, plastic products are widely used in different fields because plastic products have the characteristics of light weight, low price, high insulation, and corrosion resistance [1]. The proportion of plastic parts used in the whole vehicle is increasing, covering the exterior parts, interior parts, functional parts, and structural parts of the car [2]. In the past, the production and processing technology, which relies on experience and repeated tests of mold, has been unable to meet the needs of market development [3]. Injection molding technology can be used to quickly and efficiently obtain plastic parts, but in the process of injection molding, the quality of parts is affected by mold design, part design, materials and process parameters, and other factors [4]. Injection molding process parameters are one of the most important factors. Inappropriate parameters may result in numerous defects in the final plastic products. Therefore, it is necessary to simulate the injection molding process, optimize the product design scheme, and the process parameters of injection molding, to reduce the amount of warpage, weld lines, and other molding defects and improve the quality of the product [5].

In view of the rationality of injection molding process parameter setting, scholars in China and abroad studied the relationship between process parameters and evaluation indexes such as volume shrinkage and warpage amount by simulating the process of injection molding, so as to determine the optimal process parameters of injection molding and improve the molding quality of parts. Prasad Kumar

et al. [6] used the Taguchi L27 orthogonal array design and completed the experiment. Grey relation analysis (GRA) was used to determine the influence of process parameters on the quality of cam sleeve injection molding. The injection molding quality of the cam bush is improved by optimizing process parameters (percentage of reinforcement, nozzle temperature, injection speed, holding pressure, injection pressure, holding time, and cooling time). Park et al.[7] used the pressure and temperature sensor auxiliary monitoring system to collect real-time data. By comparing with the standard value, the relationship between parameters and plastic material properties was obtained, and the relationship between process parameters and quality failure was determined. Finally, the algorithm for compensating the deviation of process parameters was proposed. Kitayama et al. [8] took warpage amount and cycle time as evaluation indexes, and a sequential approximate optimization using a radial basis function was adopted to conduct multiobjective optimization on the pressure distribution of variable packing and four process parameters. Numerical simulation and experiments showed that this method can effectively reduce warpage amount and cycle time. Mukras et al. [9] selected seven process parameters as the test factors: mold temperature, melt temperature, packing pressure, packing time, cooling time, injection speed, and injection pressure. At the same time, the evaluation indicators were selected for warpage amount and volume shrinkage. The Kriging model between the process parameters, warpage amount, and volume shrinkage was established. A genetic algorithm was used to optimize the process parameters. The optimal process parameters were tested, and the experimental results were about 7% lower than the original results. Chauhan et al. [10] used a combination of Taguchi experimental design and Moldflow simulation to optimize process parameters, such as compression time, mold temperature, melt temperature, and pressure. The influence of process parameters on warpage amount was obtained by variance analysis, and the optimal combination of process parameters was determined by signal-to-noise ratio analysis and variance analysis. Lin and Lee [11] presented a systematic optimization procedure that integrated uniform design of experiments, Kriging interpolation, compromise programming, and generalized reduced gradient nonlinear optimization to optimize the process parameters of an injection-molded plastic wheel, which has two optimization objectives. After optimization, the maximum warpage amount and ejection time of the plastic wheel were improved by 7.7% and 11.91%, respectively. Kitayama et al. [12] determined the optimal process parameters, Pareto boundary between welds, clamping force, and cycle time by sequential approximation optimization of the radial basis function network. The variable packing curve of packing pressure change in the plastic injection molding (PIM) process was adopted to shorten the cycle time. The numerical simulation results show that the optimal pressure curve starts from the low packing pressure, and the high packing pressure is applied at the end of the packing stage. Finally, the rapid heat cycle molding (RHCM) technology is used to minimize the weld, clamping force, and cycle time, which improves the quality and efficiency of product molding. Lin et al. [13] used numerical simulation (Moldflow) to determine the flow path balance in the multicavity of a micropart. Warpage amounts were measured using various PIM process parameters (melt temperature, mold temperature, injection pressure, and fill time). Finally, the Taguchi method and grey theory are used to conclude that the most significant PIM process parameter affecting the warpage amount phenomenon of microparts is the die temperature. Silva et al. [14] compared the straight cooling channel with the conformal cooling channel and the concluded that conformal cooling channel (CCC) can obtain better cooling performance than the traditional (direct drilling) channel in the injection molding process. Wilczyrski et al. [15] proposed and discussed the latest modeling and experiments of flow and melting in injection molding machines, and concluded that some mathematical models have no strong experimental basis. Therefore, experimentation of the polymer flow and melting in the injection molding machine has been performed, and the effect of processing conditions such as the screw speed, the plasticating stroke, and the back pressure on the process course has been investigated. Speranza et al. [16] proposed a procedure that is suitable to analyze online the quality of molded parts in terms of shrinkage. The procedure allows the adoption of the pressure evolution measured by a piezoelectric pressure transducer to make an estimation of the solidification profile, thereby estimating the average solidification pressure. Eventually, the shrinkage of the part is predicted and the quality of the part is improved. Silva et al. used a random cooling system to cool the injection molding process to improve part quality. In this study, the gate position is optimized to reduce the cooling system requirements, and the relationship between the evaluation index and the gate position is established to obtain the optimal gate position and improve the forming quality of the parts. Chauhan et al. used variance analysis and signal-to-noise ratio analysis to optimize the forming process parameters, which improved the forming quality of parts, but the improvement in forming quality was not significant.

In this study, the regression equation of process parameters and evaluation indexes was obtained by a uniformity experiment, and a BP neural network combined with a genetic algorithm was used to optimize the injection molding process parameters. The optimal combination of process parameters was obtained by comparative analysis.

2. Simulation Studies of Automobile Plastic-Front End Frame

The unreasonable choice of injection molding scheme will lead to uneven filling, uneven cooling, trapped gas, and other phenomena in the injection molding process so that the injection parts have warping deformation, fusion marks, volume shrinkage, and other defects, which seriously affect the quality of injection parts [17]. By simulating the injection molding process with Moldflow, reasonable injection molding solutions can be determined, such as product material, gate location, and optimal gating system design. In this study, the establishment of the model, the selection of

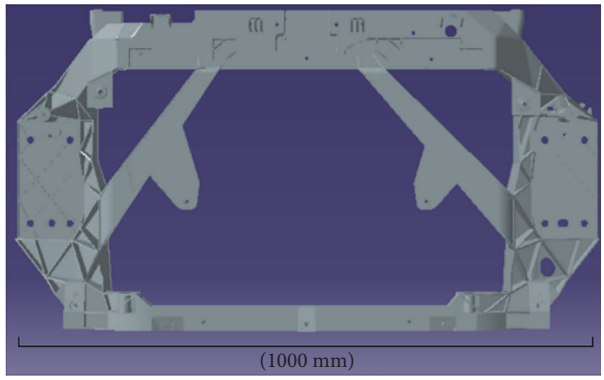

Figure 1: Automobile front-end frame model diagram.

grid division, and type, the independent verification of grid division and the best gate location are studied to provide a guarantee for the accuracy of injection molding process simulation.

2.1. The Establishment of 3D Model of Automobile Plastic Front-End Frame. The model of the automobile plastic front-end frame is established based on the original sheet metal model by using CATIA software. Under the requirements of ensuring the strength and stiffness of the parts, replacing metal parts with plastic parts can reduce the weight of the parts, thereby reducing the weight of the car. Because plastic has a smaller modulus than metal, the model takes up as much space as possible to ensure stiffness. At the same time, in order to minimize the weight of the model, the amount of material in the nonbearing area can be reduced. The model of the automobile plastic front-end frame is shown in Figure 1. The model has a complex shape with some holes around it, and the figure of eight reinforcement is used in the middle to reduce the weight of the model. The wall thickness distribution is uneven.

2.2. The Division and Type Selection of Automobile Plastic Front-End Frame Grid. The type and quality of mesh division have a great influence on the numerical simulation results; therefore, it is very important to choose the type and size of mesh reasonably [18]. The automobile plastic front-end frame studied in this study is a thin-walled product; hence, midplane mesh composed of triangular elements is used as the mesh of the model. In Hypermesh 2019 software, the mesh sizes are divided into 5 mm, 7 mm, 9 mm, 11 mm, 13 mm, and 15 mm, and the thickness of the thinnest place is 2 mm, and the thickest place is 4 mm. The long glass fiber reinforced polypropylene (PP-LGF30, that is, polypropylene contains a mass fraction of 30% of long glass fiber filling, the specific brand is Verton MV006S) was selected as the material to obtain 6 different mesh sizes. In order to improve the accuracy of the analysis results, the aspect ratio of the mesh should be controlled; that is, the maximum aspect ratio should be less than 15, and the average aspect ratio should not be more than 5. In this analysis, the maximum aspect ratio of 6.79 is far less than 15, and the average aspect ratio of 1.78 is also far less than 5. Consequently, the mesh quality meets the requirements of Moldflow analysis [19]. Taking 15 mm mesh as an example, the processed mesh model was imported into Moldflow, respectively. The mesh partitioning result was shown in Figure 2, and the mesh thickness diagnosis was shown in Figure 3.

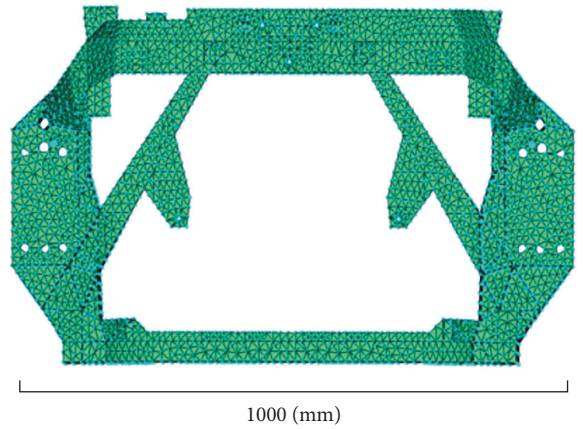

Figure 2: Front-end frame mesh model diagram.

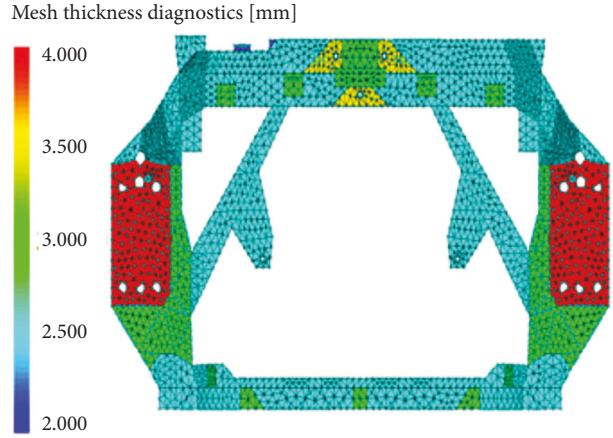

Figure 3: Mesh model thickness diagnosis diagram.

2.3. Analysis and Research on Optimum Gate Location

2.3.1. Gate Position Analysis. Moldflow is used to find the best gate position for the injection molding of parts. The gate position was selected as the analysis sequence, and the number of gates was set to 6, 7, and 8, respectively. The results of the optimum gate position analysis are shown in Figure 4. The results of gate position analysis for *a*, *b*, and *c* are 6, 7, and 8, respectively, showing the distribution of flow resistance indicators from the highest to the lowest. The blue part is the place with the lowest flow resistance, which is the best gate-setting position. The optimal gate location area recommended by gate location analysis is only for reference. In actual production, the selection of the optimal gate location also needs to consider the structural characteristics of parts and parts demoulding, exhaust, and other conditions [20].

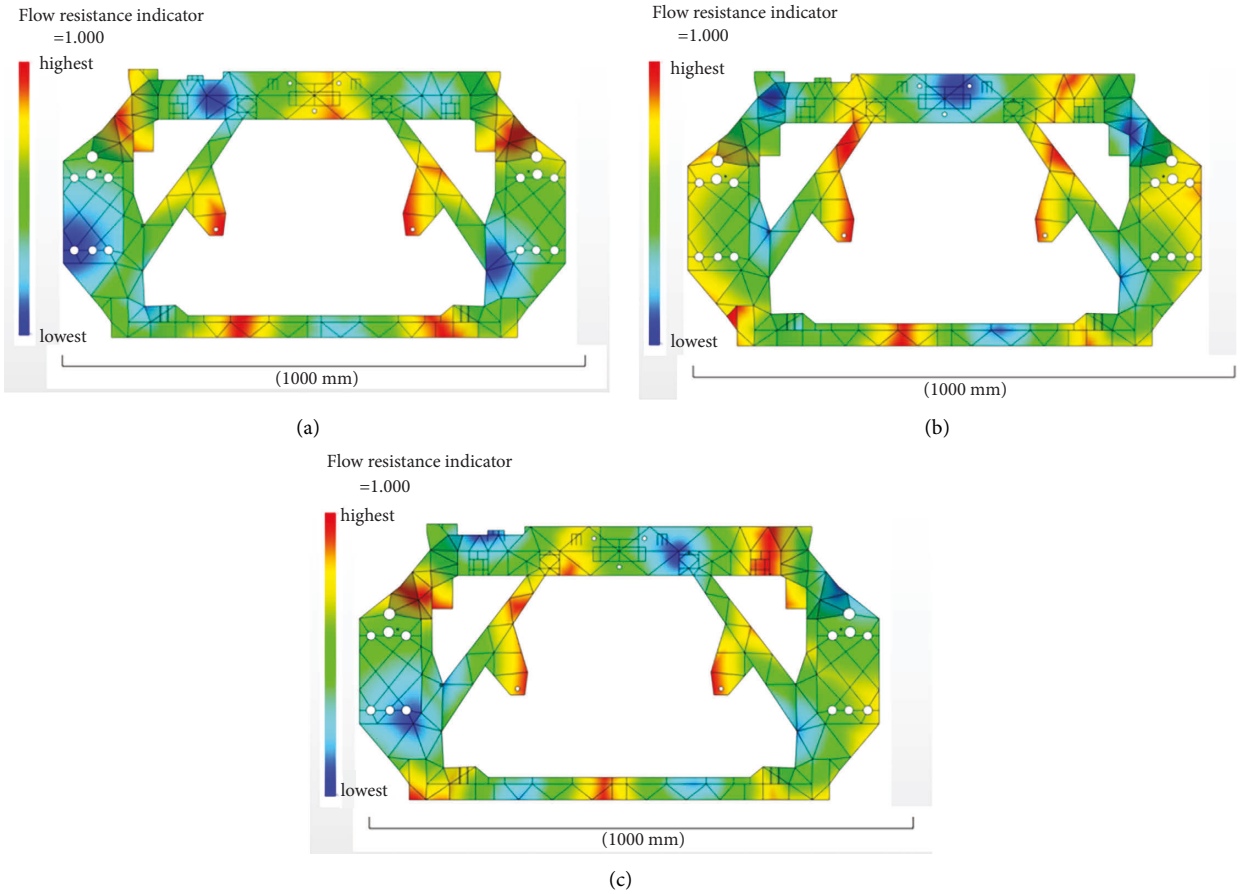

Figure 4: Optimal gate location analysis result diagram. (a) 6 gates location analysis result diagram. (b) 7 gates location analysis result diagram. (c) 8 gates location analysis result diagram.

Table 1 statistics the analysis information of different numbers of gates in mesh models with different sizes. Figure 5 shows the relationship between mesh size and mesh number, and Figure 6 shows the relationship between mesh size and analysis time. As can be seen from Figure 5, the number of meshes decreases as the mesh size increases, and as can be seen from Figure 6, the model analysis time for different gate counts decreases with the increase of the mesh size. By comparing Figures 5 and 6, it can be seen that the analysis time increases with the growth of the number of gates and the number of meshes, and the analysis time of different gates is obviously different when the mesh size is small. When the mesh size increases to 15 mm, the mesh size has little effect on the number of grids and the analysis time, so the change in the number of meshes and the analysis time tends to be gentle.

2.3.2. Optimal Gating System Design. The quality of injection parts is not only affected by injection process parameters but also by the gating system [21]. Therefore, the gating system needs to be designed before the injection molding simulation. In this study, a balanced flow channel is adopted; that is, the flow channel from the main channel to the shunt channel and then to the gate has the same section and length; hence, ensuring that the quality, structure, and performance of all parts in multicavity injection molding are the same [22]. Considering the structure of the parts and the actual production situation to determine three kinds of gating systems with pin-point gates are used. The gate settings of the upper beam and the splay beam are roughly the same for the three gating systems. Three gates are set in the upper beam, and one gate is set in each eight-word beam. The gating system of the sixth gates is set at a gate in the lower beam, the gating system of the seventh gates is set at two gates in the lower beam, and the gating system of the eighth gates is set at three gates in the lower beam.

2.3.3. Simulation Analysis of Gating System. A simulation analysis was conducted on the gating system in Figure 7. The analysis sequence is set as fill-pack-warp, and the process parameters are set as mold temperature of 50°C, melt temperature of 230°C, injection time of 2 s, pressure-packing pressure of 40 MPa, and pressure-packing time of 20 s. The cloud images of the analysis results are shown in Figures 8–10. It can be seen from Figures 8–10 that the volume shrinkage is mainly concentrated on the mounting surface of the rail because the mounting surface is thicker, and the shrinkage rate is larger in the area with a larger thickness. The warpage deformation is concentrated in the middle area of the lower beam because the material thickness

Table 1: Gate analysis information and statistical table.

Mesh size (mm)	5	7	9	11	13	15
Number of mesh (one)	124335	64028	39901	27886	20868	16379
Number of potential gates (one)	60988	31159	19202	13305	9844	7645
6 gates analysis duration (s)	3902	1501	875	575	420	305
7 gates analysis duration (s)	5578	2510	1428	883	600	431
8 gate analysis duration (s)	7715	3023	1758	1129	803	598

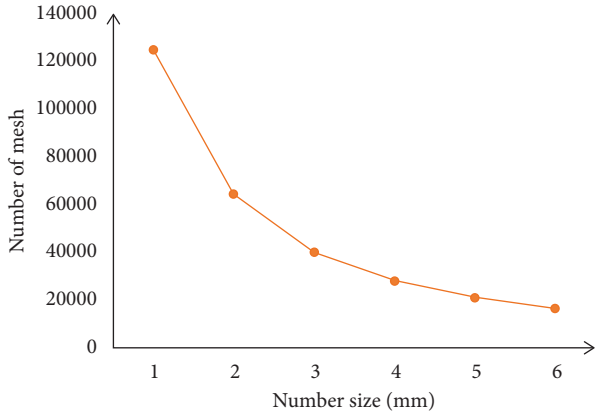

Figure 5: Mesh size and number of mesh diagrams.

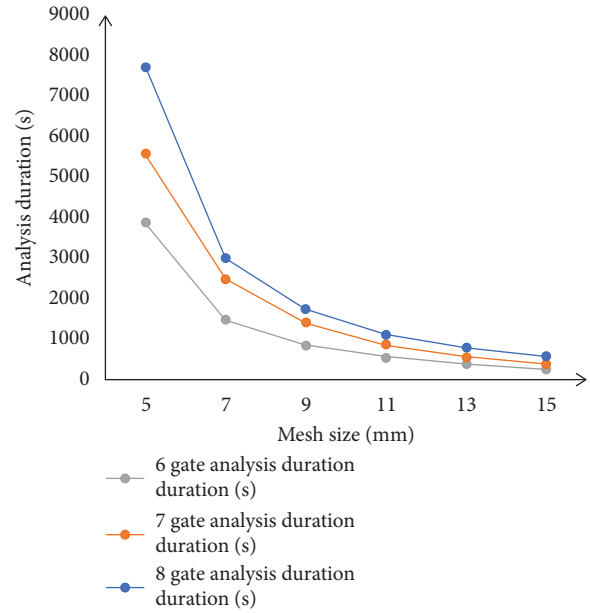

Figure 6: Mesh size and analysis time diagram.

on both sides of the front-end frame is inconsistent with that in the middle, resulting in inconsistent volume shrinkage. The stiffness of the lower beam is smaller than that of the upper beam; therefore, the warpage deformation mainly occurs in the lower beam.

2.3.4. Determination of Optimal Gating System. The quality of the gating system directly affects the quality of the parts, and the volume shrinkage, warpage amount, cavitation, and weld line shrinkage index are the evaluation indexes to measure the quality of the parts, which are affected by the gating system. Therefore, these indicators can be evaluated to measure the quality of the gating system. In this study, the simulation analysis of the parts was carried out under three different gating systems, and the values of the evaluation indexes such as volume shrinkage, warpage amount, cavitation, fusion line, and shrinkage index were obtained. Finally, these indexes were graded to obtain the optimal gating system. A comprehensive scoring method is proposed in order to determine the best gating system. Taking three kinds of gates as examples, the concrete implementation steps are as follows: first, the evaluation indexes reflecting the quality of the gating system are selected; horizontal comparison of each evaluation index; then, the gating system with the best performance in each evaluation index gets 2 points, the second one gets 1 point, and the worst one does not get any points. Finally, the scores of each gating system are added, and the system with the highest score is the best gating system.

The scoring results are shown in Table 2. Six gate gating systems get 13 points, seven gate gating systems get 8 points, and eight gate gating systems get 15 points. Therefore, the eight-gate gating system is the best gating system.

2.4. Analysis of Mesh Partition Independence. The number of meshes will affect the accuracy of the analysis results. Setting a smaller mesh size will result in more mesh numbers and more accurate analysis results, but at the same time, the analysis time will be longer [23]. When the size and number of meshing reach a certain value and then continue to increase, the influence on the calculation result is not significant, and the number of meshes is a reasonable value of meshing; that is, the size and number of meshing have nothing to do with the result [24]. In order to verify the independence of mesh division, the mesh sizes are set to 5 mm, 7 mm, 9 mm, 11 mm, 13 mm, and 15 mm, respectively. Under the same material and injection molding parameters, the automobile all-plastic front-end frames with six different mesh sizes are analyzed. The analysis results are presented in Table 3.

The influence of mesh sizes on volume shrinkage and warpage amount is shown in Figures 11 and 12. It can be seen from Figure 11 that with the increase of mesh size, the volume shrinkage tends to decrease, but the decrease degree is not large, only about 0.2%. Similarly, the effect of mesh size on warpage amount has no obvious change trend, so the size and number of divided mesh have little influence on the analysis results. Wen's research shows that the number of meshes has a certain influence on the calculation results. Under the premise of little change in the calculation results, the less the number of mesh, the better [25]. In this study, it

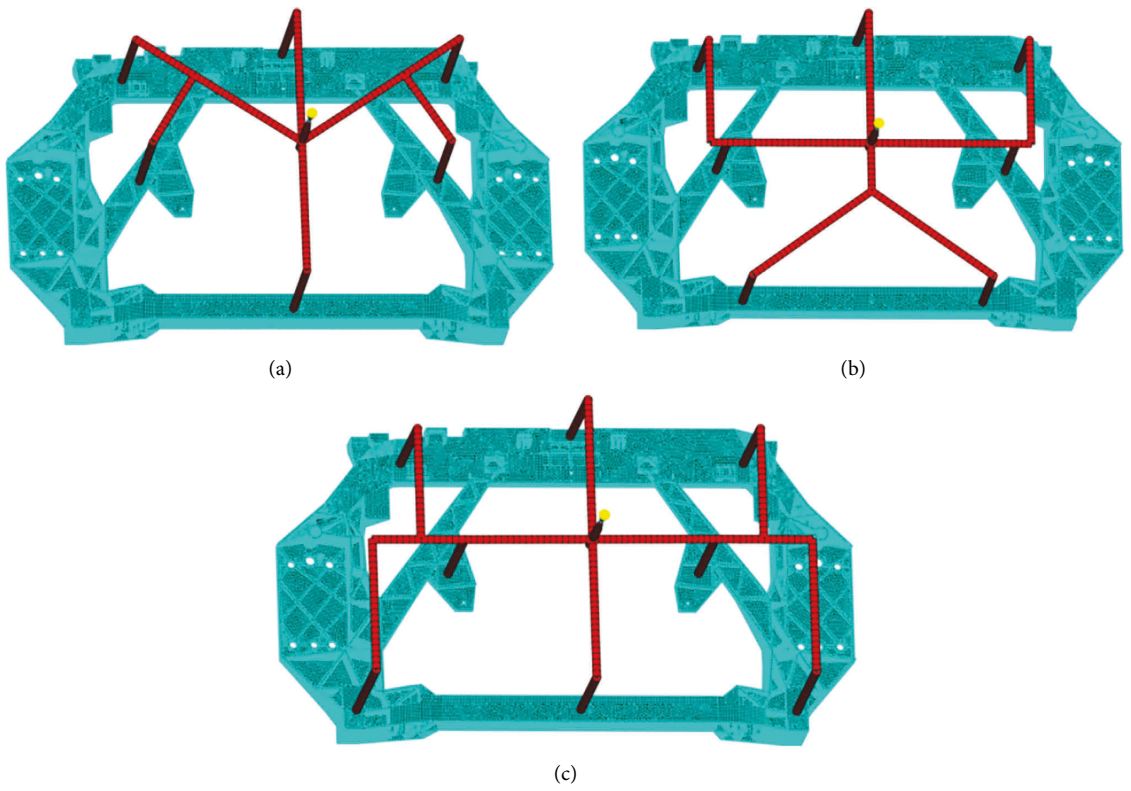

Figure 7: Gating system designed. (a) 6 gate gating systems. (b) 7 gate gating systems. (c) 8 gate gating systems.

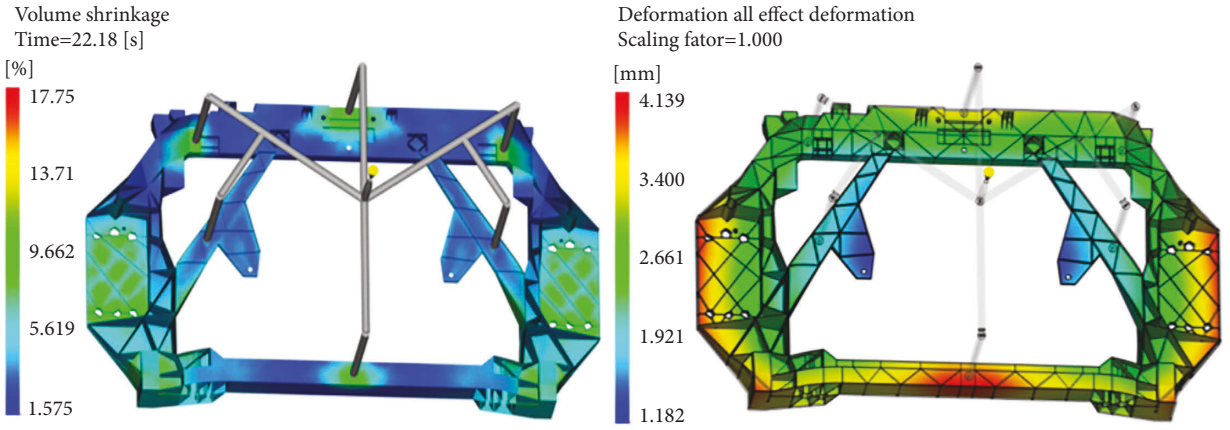

Figure 8: Volume shrinkage and warpage analysis results of the 6 gate gating systems.

is concluded that the size of the mesh division has a very small impact on the simulation, which verifies the independence of the mesh division.

3. Injection Molding Process Parameters Uniform Design Test

A uniform design experiment is a design method that considers the uniform distribution of test points in the test range. Each factor is tested once at each level. The test points of any two factors are on the grid of the plane, and there is only one test for each row and column [26]. In this study, which designs the injection molding process parameters and simulates each group, the test data for volume shrinkage and warpage amount of an automobile plastic front-end frame are obtained.

3.1. Selection of Experimental Factors and Evaluation Indexes for Uniform Design. The full plastic front-end frame of an automobile belongs to the uneven thickness of thin-walled parts, which is prone to warping deformation. In injection molding, the nonuniformity of volume shrinkage is the main cause of warping deformation [27]. Therefore, volume shrinkage and warpage amount are selected as evaluation indexes, represented by Y_1 and Y_2 respectively. There are many factors that affect the volume shrinkage and warpage deformation of parts in the molding process. Among them, mold

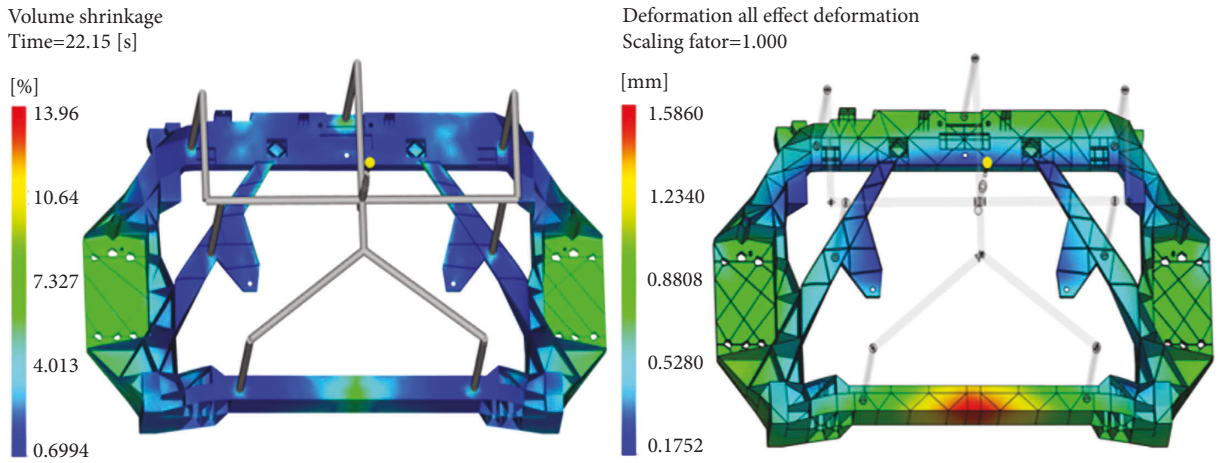

Figure 9: Volume shrinkage and warpage analysis results of the 7 gate gating systems.

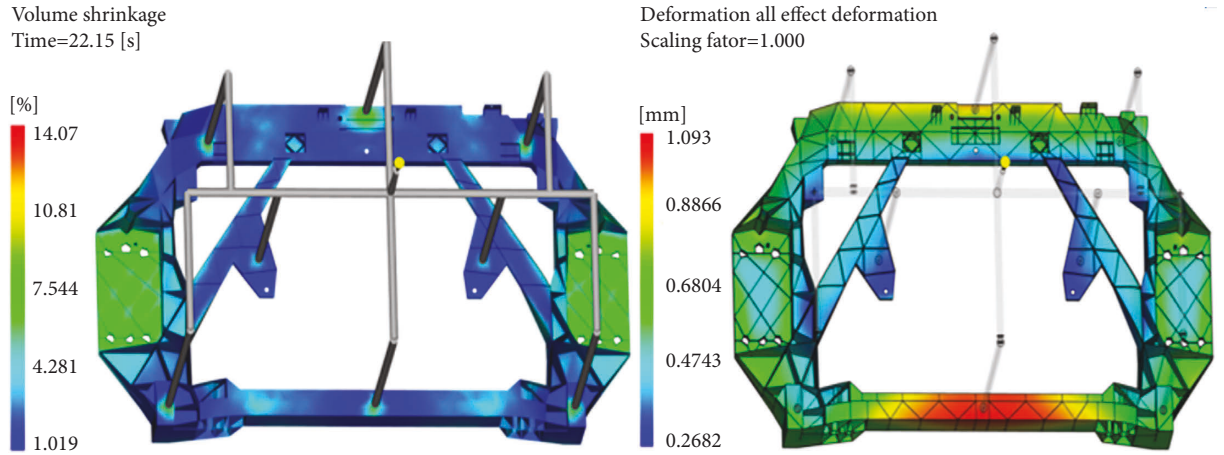

Figure 10: Volume shrinkage and warpage analysis results of the 8 gate gating systems.

Table 2: The gating system comprehensive rating table.

The evaluation index	6 gates		7 gates		8 gates	
	Amount	Score	Amount	Score	Amount	Score
Air (one)	132.00	0	122.00	1	128.00	2
Weld line (bar)	70.00	0	65.00	1	61.00	2
Sink index (%)	1.41	2	1.73	0	1.65	1
Sink mark (mm)	0.33	1	0.34	0	0.32	2
Warpage (mm)	1.37	1	1.59	0	0.92	2
Shear modulus (MPa)	1845.70	2	1841.70	1	1837.90	0
Volume shrinkage (%)	13.84	2	13.96	0	13.93	1
Shear stress at well (MPa)	0.55	1	0.46	0	0.52	2
First direction residual stress (MPa)	46.63	0	46.19	1	44.97	2
Second direction residual stress (MPa)	46.86	0	45.88	2	46.03	1
First direction tensile modulus (MPa)	10415.00	2	10388.0	1	10388.0	0
Second direction tensile modulus (MPa)	4912.60	2	4880.00	1	4845.80	0
Total points	13		8		15	

temperature, melt temperature, packing pressure, injection time, and packing time are the most influential factors [28]. The mold temperature determines the filling ability of the melt, the cooling rate of the parts, and the internal and external quality of the formed parts. Melt temperature mainly affects the plasticization and flow of plastics in injection molding. The injection time is the time needed to completely fill the mold. The size of the injection time will affect the temperature of the mold cavity and the quality and strength of the parts. Packing pressure refers to the pressure that the screw continues to maintain a certain amount of pressure over a period of time when the injection is completed. Packing time refers to the

Table 3: Statistical table of volume shrinkage and warpage analysis results of different mesh sizes.

Mesh size (mm)	Volume shrinkage (%)			Warpage (mm)		
	6 gates	7 gates	8 gates	6 gates	7 gates	8 gates
5	14.030	14.190	14.140	1.138	1.527	1.022
7	14.040	14.210	14.120	1.265	1.543	0.956
9	13.860	14.010	14.110	1.304	1.574	0.952
11	14.030	14.060	14.120	1.362	1.627	1.296
13	13.900	14.060	14.060	1.369	1.667	0.952
15	13.840	13.960	13.930	1.356	1.586	0.921

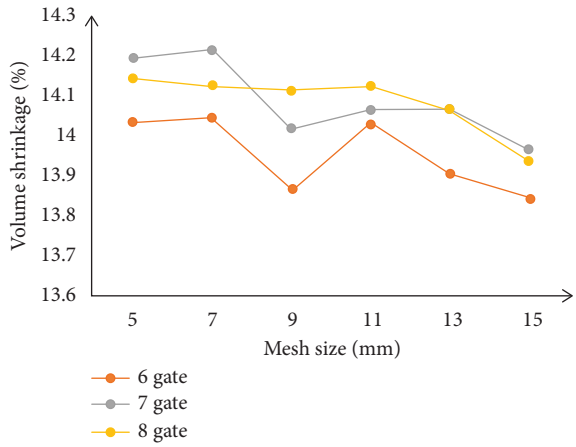

Figure 11: Diagram of mesh size and volume shrinkage.

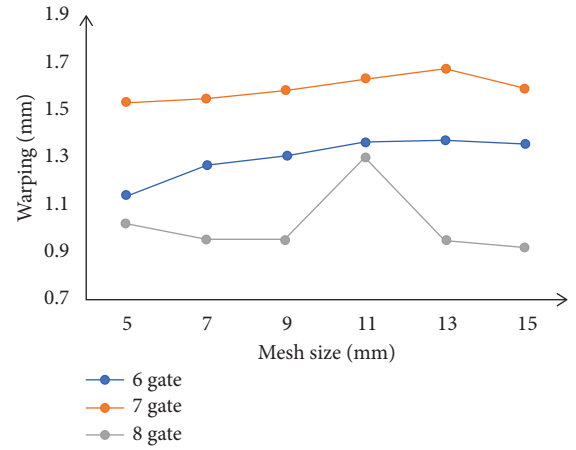

Figure 12: Diagram of mesh size and warpage.

time when the material is filled with the cavity in the injection molding under a certain pressure. Reasonable selection of packing pressure and packing time can effectively prevent shrinkage, warping deformation, and depression of parts. In this study, there are five injection process parameters: mold temperature, melt temperature, packing pressure, injection time, and packing time selected as test factors, with A, B, C, D, and E representing each test factor respectively.

3.2. Uniformly Designed Test Scheme and Simulation Results. In order to facilitate test arrangement and obtain more test results, a uniform-design test table $U_{21}^{*}(21^{5})$ is selected for the test. Select the range of process parameters according to the range of process parameters recommended by Moldflow software and the actual injection molding conditions. The selection of representative horizontal values in the test range. The test range of each process parameter is shown in Table 4. Moldflow is used to simulate injection molding for a uniform design test scheme. The results of the uniform design test scheme and injection molding simulation are presented in Table 5.

4. Optimization of Injection Molding Process Parameters Based on Regression Analysis Equation

The regression analysis method is a kind of analysis method to predict dependent variables by establishing a regression equation with good correlation by determining the relationship between dependent variables and independent variables based on the principle of data statistics [29]. Therefore, mathematical expressions can be used to characterize the relationship between evaluation indexes and process parameters. In this study, SPSS software is used to conduct multiple linear regression analysis on the results of a uniform design experiment and establish a multiple linear regression model. The regression equation is used to predict the volume shrinkage and warpage amount of the parts, and the best injection molding process parameters are obtained.

4.1. Regression Model of Volume Shrinkage. The values of A, B, C, D, E, and Y_1 in Table 5 are sequentially input into SPSS software. The regression analysis is selected, Y_1 is set as the dependent variable, and the rest are set as independent variables, and finally, the regression coefficients of each factor are obtained as shown in Table 6. The regression analysis is represented in equation (1), and the variance analysis table is shown in Table 7.

In the table, β_0 is the free regression coefficient, β_1, β_2, β_3, β_4, and β are the coefficients of factors A, B, C, D, and E, respectively.

$$R_1 = 51.46 - 0.023X_1 - 0.686X_3 - 0.032X_4 - 0.037X_5. \quad (1)$$

As expressed in equation (1), R_1 is the observed value of the regression analysis equation, and X_1, X_3, X_4, and X_5 are the values of factors A, C, D, and E in turn.

For F test in Table 7, $F_{0.001}(5, 15) = 4.56 < F = 19.85$ indicating that the regression equation is useful.

Table 4: Table of the test range of process parameters.

A (°C)	B (°C)	C (MPa)	D (s)	E (s)
70.0–90.0	230.0–446.0	40.0–50.0	2.0–5.0	20.0–60.0

Table 5: Uniform design of the test scheme and statistical table of results.

Test number	A (°C)	B (°C)	C (MPa)	D (s)	E (s)	Y_1 (%)	Y_2 (mm)
1	70.0	316.4	46.0	4.40	56.0	16.420	0.7610
2	71.0	413.6	41.5	3.65	50.0	20.0000	0.6960
3	72.0	273.2	48.0	2.90	44.0	15.5200	0.8360
4	73.0	370.4	43.5	2.15	38.0	19.4500	0.7540
5	74.0	230.0	50.0	4.70	32.0	13.3000	0.8770
6	75.0	327.2	45.5	3.95	26.0	17.0000	0.7930
7	76.0	424.4	41.0	3.20	20.0	20.6400	1.3420
8	77.0	284.0	47.5	2.45	58.0	12.9900	0.8460
9	78.0	381.2	43.0	5.00	52.0	18.2500	0.7200
10	79.0	240.8	49.5	4.25	46.0	13.8600	0.8730
11	80.0	338.0	45.0	3.50	40.0	17.6100	0.7660
12	81.0	435.2	40.5	2.75	34.0	21.3000	0.8880
13	82.0	294.8	47.0	2.00	28.0	16.6800	0.8380
14	83.0	392.0	42.5	4.55	22.0	18.8400	1.2530
15	84.0	251.6	49.0	3.80	60.0	14.4100	0.8810
16	85.0	348.8	44.5	3.05	54.0	18.2400	0.7790
17	86.0	446.0	40.0	2.30	48.0	17.9700	0.7140
18	87.0	305.6	46.5	4.85	42.0	15.9100	0.8280
19	88.0	402.8	42.0	4.10	36.0	19.4500	0.7986
20	89.0	262.4	48.5	3.35	30.0	14.9700	0.9570
21	90.0	359.6	44.0	2.60	24.0	18.8600	1.2310

Table 6: Table of regression coefficients for each factor.

Regression coefficient	β_0	β_1	β_2	β_3	β_4	β_5
Value	51.460	−0.023	0	−0.686	−0.032	−0.037

4.2. Regression Model of Warpage Amount. Columns A, B, C, D, E, and Y_2 of Table 5 in Section 3.2 are sequentially input into SPSS software. The regression analysis is selected, Y_2 is set as the dependent variable, and the rest are set as independent variables, and finally the regression coefficients of each factor are obtained as shown in Table 8. The regression analysis is represented in equation (2), and the variance analysis table is shown in Table 9.

In the table, $\beta 0$ is the free regression coefficient, β_1, β_2, β_3, β_4, and β are the coefficients of factors A, B, C, D, and E, respectively.

$$R_2 = 0.831 + 0.004X_1 + 0.001X_3 + 0.007X_4 - 0.009X_5. \quad (2)$$

As expressed in equation (2), R^2 is the observed value of the regression analysis equation, and X_1, X_3, X_4, and X_5 are the values of factors A, C, D, and E in turn.

For F test in Table 9, $F_{0.005}$ (5, 15) = 2.9 < F = 2.93, indicating that the regression equation is useful.

4.3. Regression Model Error Analysis. The experimental values of the uniform design test and the observed values calculated according to the linear regression equation are counted, as shown in Table 10, and the errors of the experimental and observed values are analyzed. The comparison between experimental and observed values is shown in Figures 13 and 14, and the errors are shown in Figures 15 and 16.

Table 7: Table of variance analysis.

Model	Sum of squares	Degrees of freedom	Mean square	F	Significant
Regression	101.847	5	20.370	19.850	**
Residual	15.393	15	1.026		
Total	117.240	20			

4.4. Optimization of Process Parameters for Volume Shrinkage. According to Table 5 in Section 3.2, group 8 has the smallest volume shrinkage, with the process following parameters: mold temperature 77°C; melt temperature 284°C; pressure-packing pressure 47.5 MPa; injection time 2.45 s; pressure-packing time 58 s. Therefore, group 8 of parameters is used as the center, and on this basis, the new range of parameters is obtained by expanding the range according to actual experience. The range of each parameter is shown in Table 11. The $U_{26}^*(26^5)$ uniform design test is conducted again in the expanded range, and formula (1) is used to predict each group of parameters. The prediction table of volume shrinkage is obtained as shown in Table 12.

As shown in Table 12, groups 5, 10, 16, 21, and 26 had the smallest volume shrinkage. Due to the possibility of error in formula (1), the combination of the five groups with the smallest volume shrinkage is selected for simulation, and the minimum volume shrinkage of group 21 is 12.61%, as shown in Figure 17. The minimum volume shrinkage is suitable for the following process parameters: mold temperature of 79°C; melt temperature of 275.6°C; packing pressure of 49.6 MPa; injection time of 2.36 s; and packing time of 57.2 s.

4.5. Optimization of Process Parameters for Warpage. According to Table 5 in Section 3.2, the warpage amount of group 2 is the smallest, and its process parameters are mold temperature of 71°C, melt temperature of 413.6°C, packing pressure of 41.5 MPa, injection time of 3.65 s, and packing pressure time of 52 s in sequence. Therefore, the second group of parameters is taken as the center, and a new range of parameters is obtained by expanding the range based on actual experience. Table 13 shows the range of parameters. The $U_{26}^*(26^5)$ uniform design test is conducted again in the expanded range, and the parameters of each group were predicted by formula (2). The warpage amount prediction table is obtained as shown in Table 14.

As shown in Table 14, the warpage amount corresponding to groups 1, 2, 3, 14, and 15 is the smallest. Due to the possibility of error in (2), the combination of the five groups with the smallest warpage amount can be selected for simulation, and the minimum warpage amount of group 3 is 0.6916 mm, as shown in Figure 18. The process parameters of minimum warping include mold temperature of 69.4°C, melt temperature of 411.8°C, packing pressure of 41.8 MPa, injection time of 3.902 s, and packing time of 51.5 s.

Table 8: Table of regression coefficients for each factor.

Regression coefficient	β_0	β_1	β_2	β_3	β_4	β_5
Value	0.831	0.004	0	0.001	0.007	−0.009

Table 9: Table of variance analysis.

Model	Sum of squares	Degrees of freedom	Mean square	F	Significant
Regression	0.293	5	0.060	2.923	*
Residual	0.351	15	0.021		
Total	0.644	20			

Table 10: Table of comparison between experimental and observed values.

Test number	Y_1 (%)	Y_2 (mm)	R_1 (%)	R_2 (mm)	$R_1 - Y_1$	$R_2 - Y_2$
1	16.4200	0.7613	16.0812	0.6838	−0.3388	−0.0775
2	20.0000	0.6957	19.3912	0.7321	−0.6088	0.0364
3	15.5200	0.8359	15.1552	0.7913	−0.3648	−0.0446
4	19.4500	0.7537	18.4652	0.8396	−0.9848	0.0859
5	13.3000	0.8767	14.1236	0.9219	0.8236	0.0452
6	17.0000	0.7926	17.4336	0.9702	0.4336	0.1776
7	20.6400	1.3420	20.7436	1.0184	0.1036	−0.3236
8	12.9900	0.8455	14.8796	0.6817	1.8896	−0.1639
9	18.2500	0.7200	18.0840	0.7530	−0.1660	0.0330
10	13.8600	0.8730	13.848	0.8123	−0.0120	−0.0608
11	17.6100	0.7664	17.1580	0.8605	−0.4520	0.0941
12	21.3000	0.8837	20.4680	0.9088	−0.8320	0.02505
13	16.6800	0.8375	16.2320	0.9680	−0.4480	0.1305
14	18.8400	1.2530	19.4364	1.0394	0.5964	−0.2137
15	14.4100	0.8804	13.5724	0.7026	−0.8376	−0.1778
16	18.2400	0.7790	16.8824	0.7509	−1.3576	−0.0282
17	17.9700	0.7135	20.1924	0.7991	2.2224	0.0856
18	15.9100	0.8279	15.8508	0.8815	−0.0592	0.0536
19	19.4500	0.7986	19.1608	0.9297	−0.2892	0.1311
20	14.9700	0.9568	14.9248	0.9890	−0.0452	0.0322
21	18.8600	1.2310	18.2348	1.0372	−0.6252	−0.1938

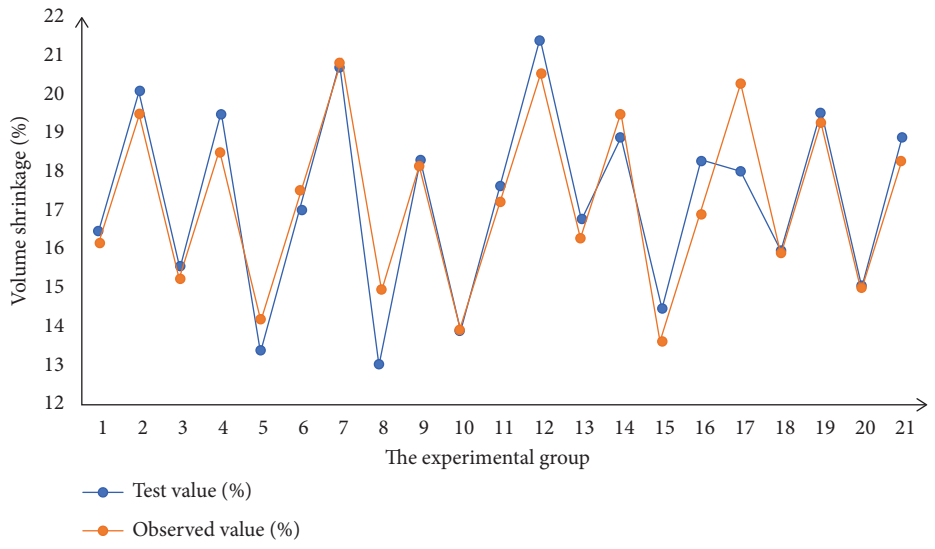

Figure 13: Comparison of experimental and observed volume shrinkage values.

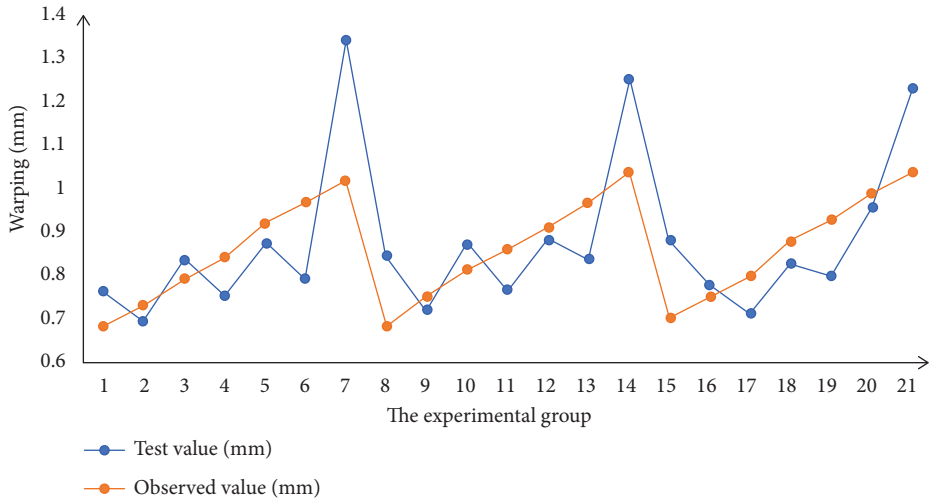

Figure 14: Comparison of experimental and observed warpage values.

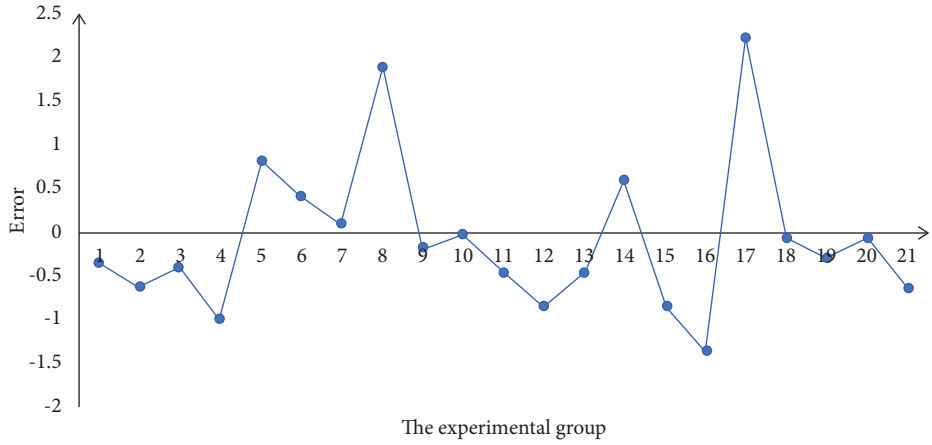

Figure 15: Volume shrinkage error diagram.

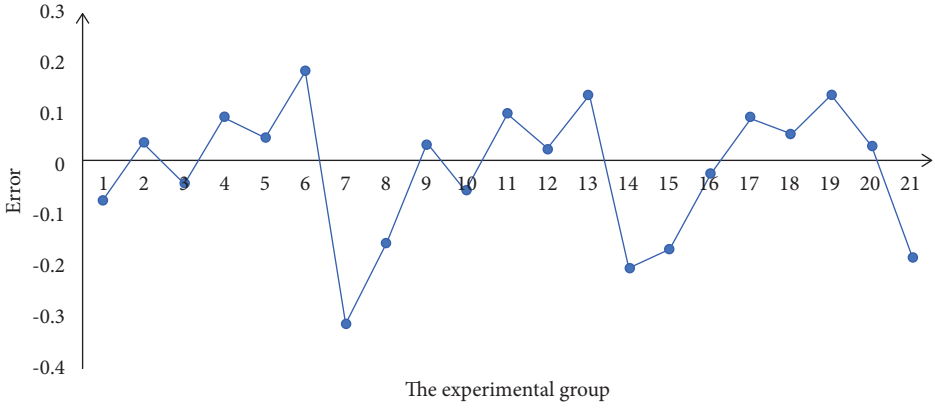

Figure 16: Warpage error diagram.

Table 11: Table of parameter ranges.

A (°C)	B (°C)	C (MPa)	D (s)	E (s)
75.0–80.0	274.0–394.0	45.0–50.0	2.3.0–2.6.0	55.0–60.0

Table 12: Volume shrinkage prediction table.

Test number	A (°C)	B (°C)	C (MPa)	D (s)	E (s)	R_1' (%)
1	75.0	276.4	45.8	2.492	59.8	16.0239
2	75.2	279.6	46.8	2.372	59.4	15.3519
3	75.4	282.8	47.8	2.576	59.0	14.6696
4	75.6	286.0	48.8	2.456	58.6	13.9976
5	75.8	289.2	49.8	2.336	58.2	13.3256
6	76.0	292.4	45.4	2.540	57.8	16.3477
7	76.2	274.0	46.4	2.420	57.4	15.6758
8	76.4	277.2	47.4	2.300	57.0	15.0038
9	76.6	280.4	48.4	2.504	56.6	14.3215
10	76.8	283.6	49.4	2.384	56.2	13.6495
11	77.0	286.8	45.0	2.588	55.8	16.6716
12	77.2	290.0	46.0	2.468	55.4	15.9996
13	77.4	293.2	47.0	2.348	55.0	15.3277
14	77.6	274.8	48.0	2.552	60.0	14.4455
15	77.8	278.0	49.0	2.432	59.6	13.7736
16	78.0	281.2	50.0	2.312	59.2	13.1016
17	78.2	284.4	45.6	2.516	58.8	16.1237
18	78.4	287.6	46.6	2.396	58.4	15.4517
19	78.6	290.8	47.6	2.600	58.0	14.7694
20	78.8	294.0	48.6	2.480	57.6	14.0974
21	79.0	275.6	49.6	2.360	57.2	13.4255
22	79.2	278.8	45.2	2.564	56.8	16.4476
23	79.4	282.0	46.2	2.444	56.4	15.7756
24	79.6	285.2	47.2	2.324	56.0	15.1036
25	79.8	288.4	48.2	2.528	55.6	14.4213
26	80.0	291.6	49.2	2.408	55.2	13.7493

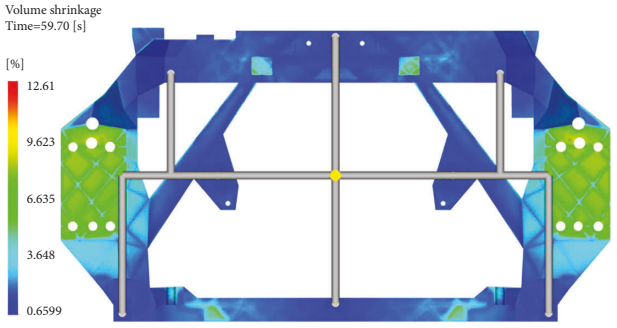

Figure 17: Acloud map of minimum volume shrinkage.

Table 13: Table of parameter ranges.

A (°C)	B (°C)	C (MPa)	D (s)	E (s)
69.0–74.0	403.0–423.0	39.0–44.0	3.35–3.95	47.5–52.5

Table 14: Volume shrinkage prediction table.

Test number	A (°C)	B (°C)	C (MPa)	D (s)	E (s)	R_2' (mm)
1	69.0	405.4	39.8	3.734	52.3	0.7023
2	69.2	408.6	40.8	3.494	51.9	0.7060
3	69.4	411.8	41.8	3.902	51.5	0.7142
4	69.6	415.0	42.8	3.662	51.1	0.7179
5	69.8	418.2	43.8	3.422	50.7	0.7217
6	70.0	421.4	39.4	3.830	50.3	0.7245
7	70.2	403.0	40.4	3.590	49.9	0.7282
8	70.4	406.2	41.4	3.350	49.5	0.7320
9	70.6	409.4	42.4	3.758	49.1	0.74021
10	70.8	412.6	43.4	3.518	48.7	0.7439
11	71.0	415.8	39.0	3.926	48.3	0.7468
12	71.2	419.0	40.0	3.686	47.9	0.7505
13	71.4	422.2	41.0	3.446	47.5	0.7542
14	71.6	403.8	42.0	3.854	52.5	0.7139
15	71.8	407.0	43.0	3.614	52.1	0.7176
16	72.0	410.2	44.0	3.374	51.7	0.7213
17	72.2	413.4	39.6	3.782	51.3	0.7242
18	72.4	416.6	40.6	3.542	50.9	0.7279
19	72.6	419.8	41.6	3.95	50.5	0.7362
20	72.8	423.0	42.6	3.71	50.1	0.7399
21	73.0	404.6	43.6	3.47	49.7	0.7436
22	73.2	407.8	39.2	3.878	49.3	0.7465
23	73.4	411.0	40.2	3.638	48.9	0.7502
24	73.6	414.2	41.2	3.398	48.5	0.7539
25	73.8	417.4	42.2	3.806	48.1	0.7621
26	74.0	420.6	43.2	3.566	47.7	0.7659

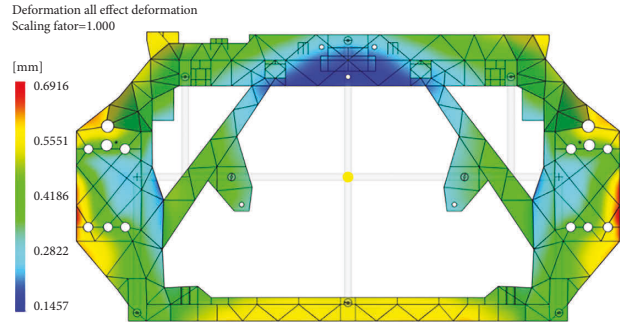

Figure 18: Acloud map of minimum warpage.

5. Optimization of Injection Molding Process Parameters Based on BP Neural Network and Genetic Algorithm

Using a linear regression equation to express the functional relationship between process parameters and evaluation indexes can only obtain local optimal process parameters, which cannot optimize the two evaluation indexes at the same time. The combination of a aBP neural network and a genetic algorithm can carry out multiobjective optimization and a obtain global optimal solution. Therefore, this chapter builds a neural network model whose input is the process parameter and whose output is the evaluation index. The weights and thresholds of the neural network model are optimized by the genetic algorithm, and it is used to predict the corresponding process parameters when the evaluation index is optimal. The combination of a BP neural network and a genetic algorithm can realize multiobjective optimization and obtain a global optimal solution.

5.1. Processing of Test Data. As a large amount of data is needed to build the neural network, the Moldflow simulated data of groups 5, 10, 16, 21, and 26 in Table 12 in Section 4.4 and groups 1, 2, 3, 14, and 15 in Table 14 in Section 4.5 are summarized into the experimental design table, and Table 15 is obtained. In order to obtain more accurate optimization results, three levels are taken for each factor, and a comprehensive design test is designed. The specific level values are shown in Table 16. The comprehensive design experiment is simulated, and 243 groups of test data are obtained.

5.2. The Establishment of BP Neural Network Model. The BP neural network is a multilayer feedforward neural network trained according to the error reverse propagation algorithm [30]. This network generally consists of three or more neuron layers, namely a single input layer, an output layer, and multiple hidden layers. In this study, a three-layer network with an input layer, an output layer, and a hidden layer is adopted. The number of nodes in the input layer is the number of process parameters, and the number of nodes in the output layer is the number of evaluation indexes. According to the prediction error and convergence speed, the number of nodes in the hidden layer is determined to be 15 after several tests. The BP neural network model with five inputs and two outputs is established by MATLAB with five input and two output parameters as input and volume shrinkage and warpage amount as output. The structure diagram of the BP neural network model is shown in Figure 19.

5.3. The Prediction Error Analysis of the Model. After the establishment of the BP neural network model, the model needs to be trained to make the model more accurately approximate the functional relationship between process parameters and evaluation indexes. A comprehensive design experiment is used as a training group, and the 31 sets of data in Table 15 are used as test groups. Volume shrinkage test results are shown in Figure 20, warpage amount test results are shown in Figure 21, and the prediction error is shown in Figures 22 and 23.

It can be seen from Figures 20 and 21 that the established BP neural network model can roughly predict the output result according to the input. It can be seen from Figures 22 and 23 that the prediction error of the BP neural network for the volume shrinkage is better than that of the warpage deformation.

5.4. Genetic Algorithm Optimized BP Neural Network Model. A genetic algorithm is a kind of algorithm that simulates the rules of biological evolution by computer. The range of optimization corresponds to the genetic space, and the coding is carried out through binary codes. Each group of codes is evaluated according to the expected results and the most appropriate value is selected [31]. A genetic algorithm is used to binary code the total number of nodes of the weight and threshold value, and process them through selection, crossover, and variogram until the error between the output value of the weight and threshold value and the real value is less than the set error. After the weights and thresholds are reassigned to the BP neural network model, the test group can be used to test the new neural network model. The test results of volume shrinkage and warpage amount are shown in Figures 24 and 25, and the prediction errors are shown in Figures 26 and 27.

It can be seen from the figure that the test error of the BP neural network optimized by a genetic algorithm is greatly reduced. Two neural network model pairs are shown in Table 17.

As shown in Table 17, the modeling time of the BP neural network optimized by a genetic algorithm is significantly shortened, and the mean square error of volume shrinkage rate and warpage amount are both reduced, which indicates that the optimization results are good and can be used for subsequent prediction.

Table 15: Test data sheet.

Test number	A (°C)	B (°C)	C (MPa)	D (s)	E (s)	Y_1 (%)	Y_2 (mm)
1	70.0	316.4	46.0	4.400	56.0	16.42	0.7613
2	71.0	413.6	41.5	3.650	50.0	20.00	0.6957
3	72.0	273.2	48.0	2.900	44.0	15.52	0.8359
4	73.0	370.4	43.5	2.150	38.0	19.45	0.7537
5	74.0	230.0	50.0	4.700	32.0	13.30	0.8767
6	75.0	327.2	45.5	3.950	26.0	17.00	0.7926
7	76.0	424.4	41.0	3.200	20.0	20.64	1.3420
8	77.0	284.0	47.5	2.450	58.0	12.99	0.8455
9	78.0	381.2	43.0	5.000	52.0	18.25	0.7200
10	79.0	240.8	49.5	4.250	46.0	13.86	0.8730
11	80.0	338.0	45.0	3.500	40.0	17.61	0.7664
12	81.0	435.2	40.5	2.750	34.0	21.30	0.8837
13	82.0	294.8	47.0	2.000	28.0	16.68	0.8375
14	83.0	392.0	42.5	4.550	22.0	18.84	1.2530
15	84.0	251.6	49.0	3.800	60.0	14.41	0.8804
16	85.0	348.8	44.5	3.050	54.0	18.24	0.7790
17	86.0	446v	40.0	2.300	48.0	17.97	0.7135
18	87.0	305.6	46.5	4.850	42.0	15.91	0.8279
19	88.0	402.8	42.0	4.100	36.0	19.45	0.7986
20	89.0	262.4	48.5	3.350	30.0	14.97	0.9568
21	90.0	359.6	44.0	2.600	24.0	18.86	1.2310
22	75.8	289.2	49.8	2.336	58.2	13.00	0.8617
23	76.8	283.6	49.4	2.384	56.2	12.86	0.8355
24	78.0	281.2	50.0	2.312	59.2	12.71	0.8366
25	78.8	294.0	48.6	2.480	57.6	12.61	0.8463
26	80.0	291.6	49.2	2.408	55.2	13.17	0.8283
27	69.0	405.4	39.8	3.734	52.3	19.70	0.7079
28	69.2	408.6	40.8	3.494	51.9	19.94	0.7047
29	69.4	411.8	41.8	3.902	51.5	19.79	0.6916
30	71.6	403.8	42.0	3.854	52.5	19.56	0.7005
31	71.8	407.0	43.0	3.614	52.1	19.81	0.6969

Table 16: Comprehensive design of test level table.

Level	A (°C)	B (°C)	C (MPa)	D (s)	E (s)
1	70.0	230.0	40.0	2.0	20.0
2	80.0	338.0	45.0	3.5	40.0
3	90.0	446.0	50.0	5.0	60.0

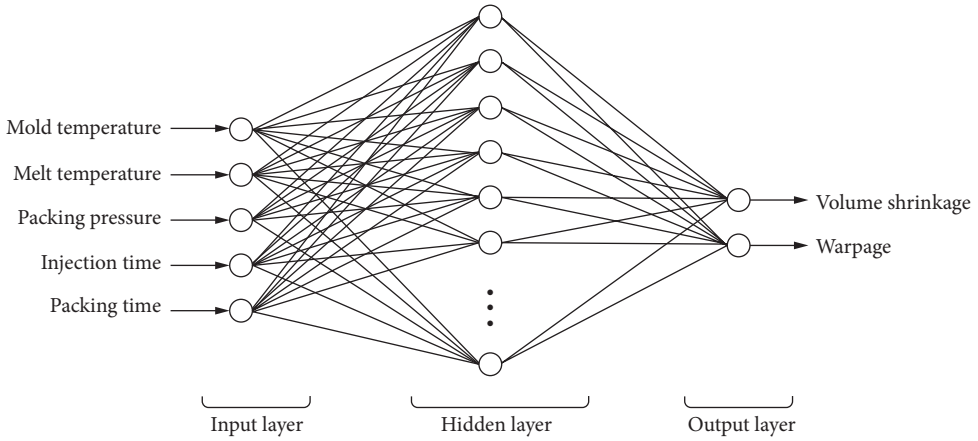

Figure 19: Structure diagram of BP neural network model.

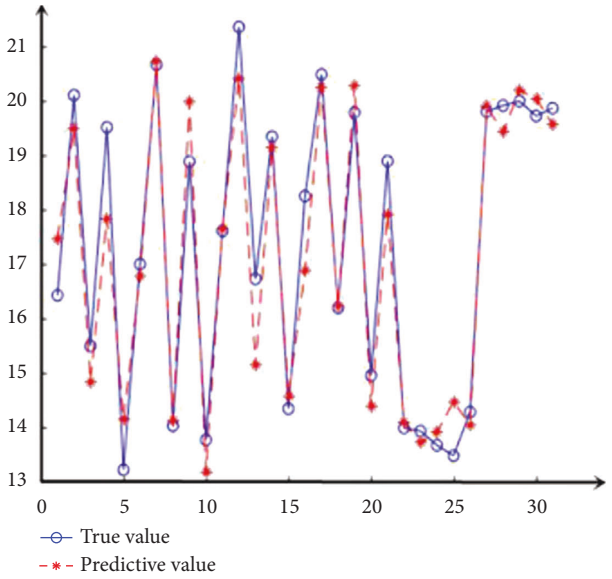

Figure 20: Figure of predicted results of volume shrinkage.

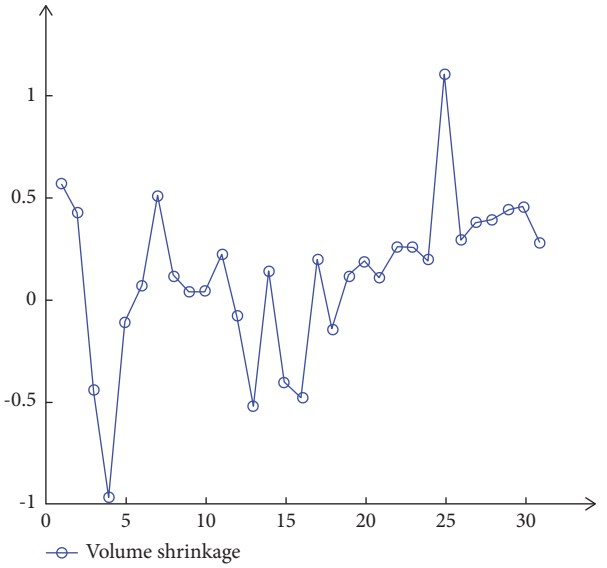

Figure 22: Volume shrinkage prediction error chart.

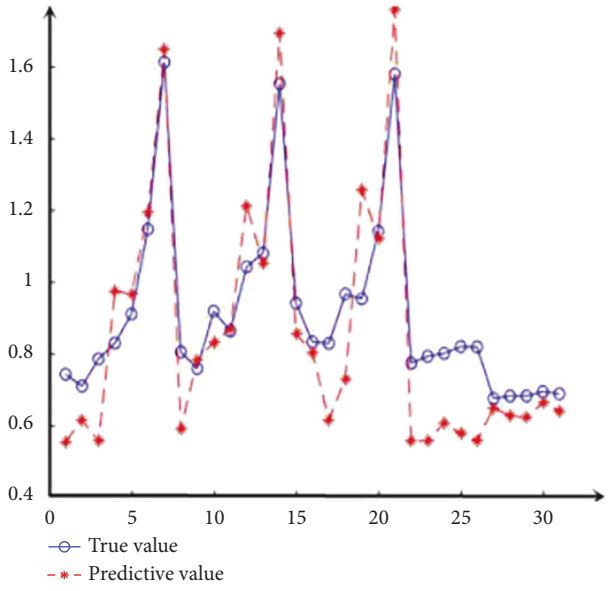

Figure 21: Warpage prediction result diagram.

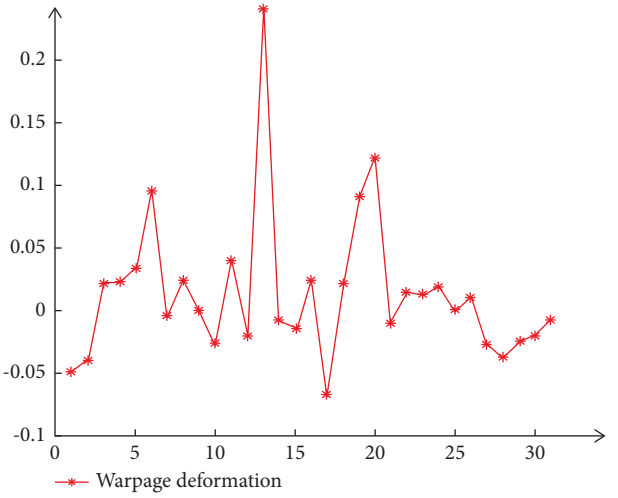

Figure 23: Warpage prediction error diagram.

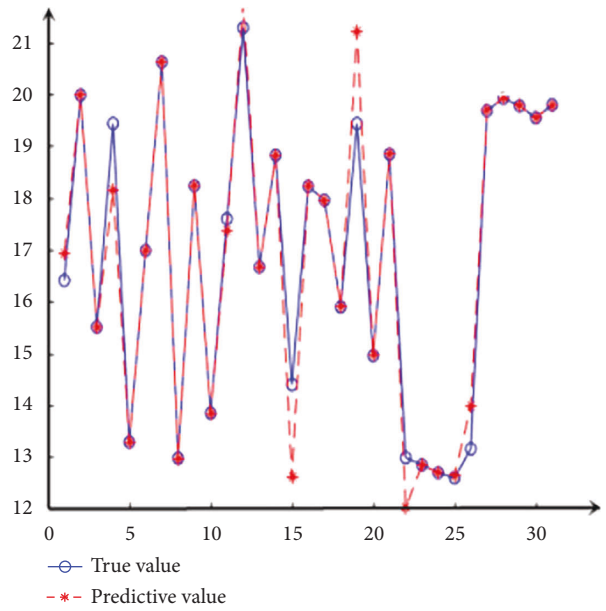

Figure 24: Optimized volume shrinkage test diagram.

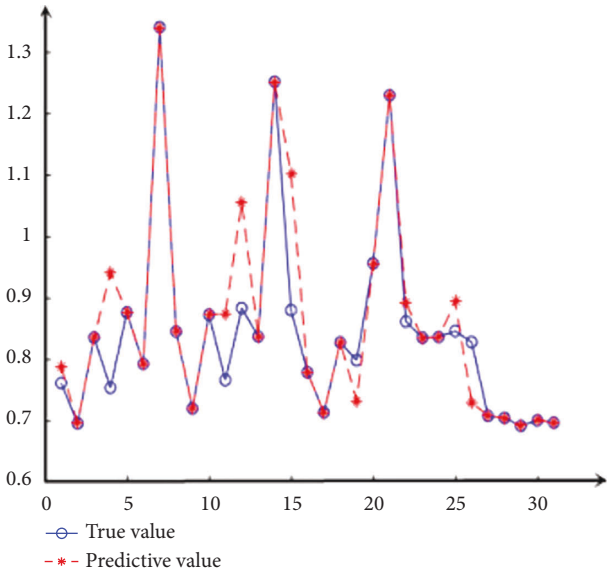

Figure 25: Optimized warpage test diagram.

5.5. Determination of Optimum Process Parameters. In the range of each process parameter, the predicted value of volume shrinkage and warpage amount is set as the minimum, and the optimized BP neural network is used to predict. In the range of each process parameter, the predicted value of volume shrinkage and warpage amount is set as the minimum, and the optimized BP neural network is used to predict. The predicted volume shrinkage rate is 12.95%, the warping amount is 0.713 mm, and the corresponding technological parameters are mold temperature of 75.5°C, melt temperature of 285.32°C, packing pressure of 42.32 MPa, injection time of 3.45 s, and packing

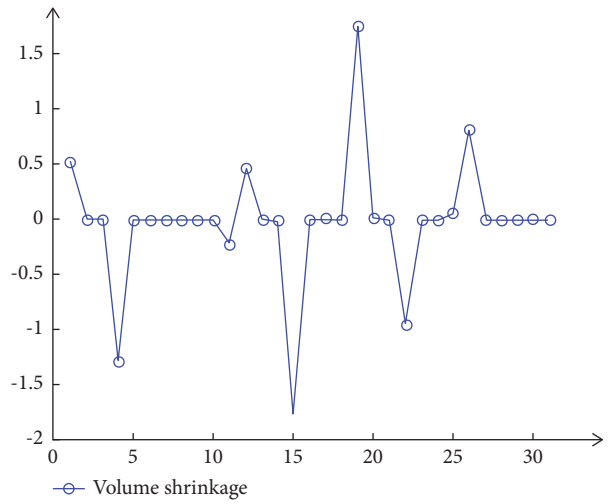

Figure 26: Optimized volume shrinkage error diagram.

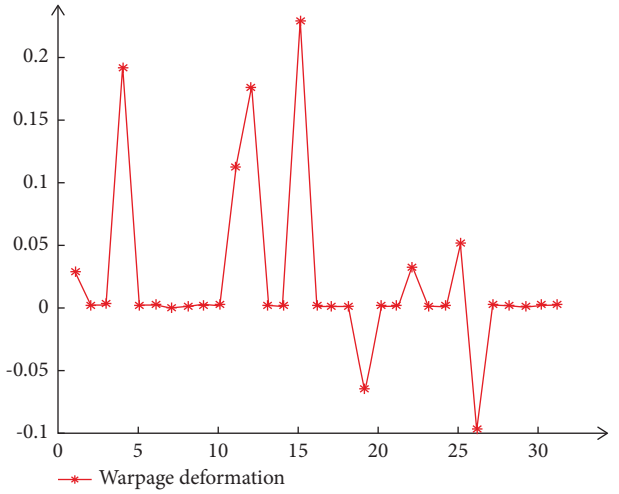

Figure 27: Optimized Warpage error diagram.

Table 17: Comparison table of neural network models before and after optimization.

	Modeling time (s)	Mean square error of volume shrinkage	Mean square error of warpage
Pre-optimized BP neural network	5.3352	1.5670	0.9865
Optimization of BP neural network by GA	0.2340	0.1258	0.0421

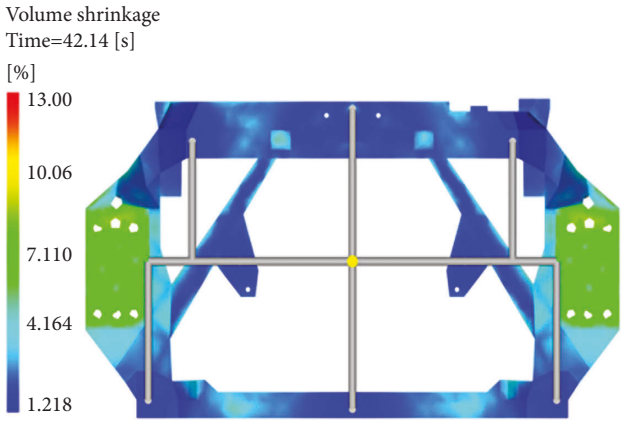

Figure 28: Cloud image of volume shrinkage.

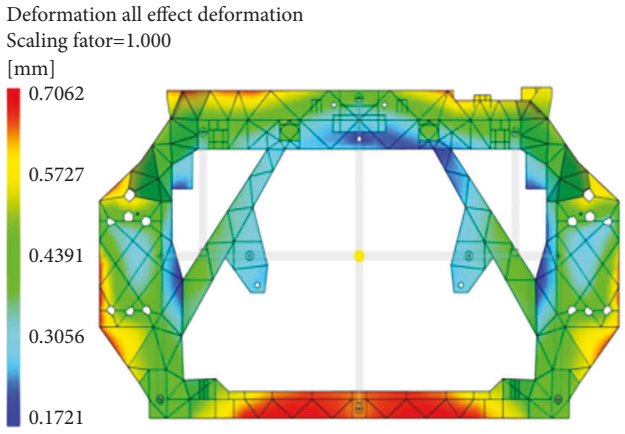

Figure 29: Cloud image of warpage.

time of 60 s. Each process parameter was input into Moldflow for verification, and the volume shrinkage rate and warpage amount obtained are shown in Figures 28 and 29. Through Moldflow verification, the corresponding volume shrinkage rate of this group of parameters is 13%, and the warpage amount is 0.7062 mm. There is no significant difference between the verified results and the predicted results. Using an optimized BP neural network to predict the global optimal solution, the predicted process parameters can make the volume shrinkage and warpage amount reach the optimal state at the same time, while they cannot reach the minimum at the same time.

6. Conclusions

In this study, the injection molding process parameters optimization of the automobile front-end frame was studied. Five process parameters, including mold temperature, melt temperature, packing pressure, injection time, and packing time, were selected as experimental factors, and volume shrinkage and warpage amount were selected as evaluation indexes. The uniformity experiment was designed and completed. The injection molding process parameters of the automobile front-end frame were optimized by using a regression equation, a genetic algorithm, and a BP neural network model. The results show that

(1) By evaluating the gating systems of 6, 7, and 8 gates, the optimum gating system was determined as 8 gate gating systems. Through the simulation of the injection molding process parameters recommended by the software, the values of volume shrinkage and warpage amount were obtained as 13.93% and 0.9204 mm, respectively.

(2) The regression equation was used to optimize the volume shrinkage and warpage amount. The minimum volume shrinkage of the optimized product was 12.61%, and the warpage amount was 0.8127 mm. The corresponding parameters were as follows: mold temperature of 79°C; melt temperature of 275.6°C; holding pressure of 49.6 MPa; injection time of 2.36 s; and holding time of 57.2 s. The minimum warpage amount was 0.6916 mm, and the volume shrinkage was 19.16% mm. The corresponding parameters were as follows: mold temperature of 69.4°C; melt temperature of 411.8°C; holding pressure of 41.8 MPa; injection time of 3.902 s; and holding time of 51.5 s. Compared with before optimization, the volume shrinkage and warpage amount are reduced to a certain extent, but they cannot reach the optimal state at the same time.

(3) Finally, the genetic algorithm and the BP neural network model were used to simultaneously optimize the volume shrinkage and warpage amount. The volume shrinkage and warpage amount of the optimized parts were 13% and 0.7062 mm, respectively. The corresponding process parameters were as follows: mold temperature of 75.5°C, melt temperature of 285.32°C, holding pressure of 42.32 MPa, injection time of 3.45 s, and holding time of 60 s. After optimization, the volume shrinkage and warpage amount of the vehicle's plastic front-end frame reach the optimal state.

(4) Based on the optimization of the regression equation, the volume shrinkage and warpage amounts were reduced by 1.35% and 0.1077 mm, respectively. Based on the optimization of the BP neural network and genetic algorithm, the volume shrinkage and warpage amount were decreased by 0.93% and 0.2142 mm, respectively. Therefore, the use of the BP neural network and a genetic algorithm was beneficial to improve the forming quality of the parts.

Through the research on the all-plastic front-end frame of an automobile, the quality and efficiency of injection molding were improved, and the processing cost of manufacturers was reduced, which has certain guiding significance for the injection molding industry. In the future, more factors (such as cooling time, injection pressure, clamping force, etc.) can be considered to affect the quality of parts, and more objectives such as weld line, shrinkage index, and residual stress can be optimized to further improve the quality of parts.

Data Availability

The data used to support the findings of this study are included within the article.

Conflicts of Interest

The authors declare that they have no conflicts of interest.

Acknowledgments

This article belongs to the major projects of the "The University Synergy Innovation Program of Anhui Province (GXXT-2019-004)." This article belongs to the project of the "Teaching Research Project of Anhui Education Department (2019jyxm0229)." Science and Technology Planning Project of Wuhu City, 2021YF58.

References

[1] H. Radhwan, S. M. Nasir, M. M. Rashidi, K. Kamarudin, and A. Abdellah, "Optimization parameters to reduce the warpage defect of plastic injection molding process for a thin-shell part using design of experiment," *IOP Conference Series: Materials Science and Engineering*, vol. 551, no. 1, Article ID 012027, 2019.

[2] H. Mao, Y. Wang, and D. Yang, "Study of injection molding process simulation and mold design of automotive back door panel," *Journal of Mechanical Science and Technology*, vol. 36, no. 5, pp. 2331–2344, 2022.

[3] R. J. Bensingh, R. Machavaram, S. R. Boopathy, and C. Jebaraj, "Injection molding process optimization of a bi-aspheric lens using hybrid artificial neural networks (ANNs) and particle swarm optimization (PSO)," *Measurement*, vol. 134, pp. 359–374, 2019.

[4] M. Moayyedian, K. Abhary, and R. Marian, "Optimization of injection molding process based on fuzzy quality evaluation and Taguchi experimental design," *CIRP journal of manufacturing Science and technology*, vol. 21, pp. 150–160, 2018.

[5] F. Hentati, I. Hadriche, N. Masmoudi, and C Bradai, "Optimization of the injection molding process for the PC/ABS parts by integrating Taguchi approach and CAE simulation," *International Journal of Advanced Manufacturing Technology*, vol. 104, no. 9-12, pp. 4353–4363, 2019.

[6] B. Prasad Kumar, P. Venkataramaiah, and J. Siddi Ganesh, "Optimization of process parameters in injection moulding of A polymer composite product by using g," *Materials Today Proceedings*, vol. 18, pp. 4637–4647, 2019.

[7] H. S. Park, D. X. Phuong, and S. Kumar, "AI based injection molding process for consistent product quality," *Procedia Manufacturing*, vol. 28, pp. 102–106, 2019.

[8] S. Kitayama, M. Yokoyama, M. Takano, and S. Aiba, "Multi-objective optimization of variable packing pressure profile and process parameters in plastic injection molding for minimizing warpage and cycle time," *International Journal of Advanced Manufacturing Technology*, vol. 92, no. 9-12, pp. 3991–3999, 2017.

[9] S. M. S. Mukras, H. M. Omar, and F. A. al-Mufadi, "Experimental-based multi-objective optimization of injection molding process parameters," *Arabian Journal for Science and Engineering*, vol. 44, no. 9, pp. 7653–7665, 2019.

[10] V. Chauhan, T. Kärki, and J. Varis, "Optimization of compression molding process parameters for NFPC manufacturing using taguchi design of experiment and moldflow analysis," *Processes*, vol. 9, no. 10, p. 1853, 2021.

[11] P. C. Lin and C. K. Lee, "Process Parameters Optimization for an Injection-Molded Plastic Wheel by Uniform Design of experiment and Kkriging interpolation," *DEStech Transactions on Engineering and Technology Research*, vol. 2, no. 3, 2017.

[12] S. Kitayama, S. Tsurita, M. Takano, Y. Yamazaki, Y. Kubo, and S. Aiba, "Multi-objective process parameters optimization in rapid heat cycle molding incorporating variable packing pressure profile for improving weldline, clamping force, and cycle time," *International Journal of Advanced Manufacturing Technology*, vol. 120, no. 5-6, pp. 3669–3681, 2022.

[13] W. C. Lin, F. Y. Fan, C. F. Huang, Y. K. Shen, and H. Wang, "Analysis of the warpage phenomenon of micro-sized parts with precision injection molding by experiment, numerical simulation, and grey theory," *Polymers*, vol. 14, no. 9, p. 1845, 2022.

[14] H. M. Silva, J. T. Noversa, L. Fernandes, H. L. Rodrigues, and A. J. Pontes, "Design, simulation and optimization of conformal cooling channels in injection molds: a review," *International Journal of Advanced Manufacturing Technology*, vol. 120, no. 7-8, pp. 4291–4305, 2022.

[15] K. Wilczyński, K. J. Wilczyński, and K. Buziak, "Modeling and experimental studies on polymer melting and flow in injection molding," *Polymers*, vol. 14, no. 10, p. 2106, 2022.

[16] V. Speranza, U. Vietri, and R. Pantani, "Adopting the experimental pressure evolution to monitor online the shrinkage in injection molding," *Industrial & Engineering Chemistry Research*, vol. 51, no. 49, Article ID 16034, 2012.

[17] H. Wang and C. Sun, "Gate optimization analysis of injection molding for mobile phone panel based on moldflow and drop simulation," *World Journal of Engineering and Technology*, vol. 09, no. 1, pp. 92–99, 2021.

[18] M. Abobaker, S. Addeep, L. O. Afolabi, and M E. Abdulhafid, "Effect of mesh type on numerical computation of aerodynamic coefficients of NACA 0012 a," *Journal of Advanced Research in Fluid Mechanics and Thermal Sciences*, vol. 87, no. 3, pp. 31–39, 2021.

[19] Y. C. Chen, S. L. Wang, and Y. H. Wang, "Ram injection molding mold flow analysis and process parameter optimization," *The International Journal of Oral Implantology*, vol. 7, no. 4, p. 165, 2015.

[20] H. Wu, Y. Wang, and M. Fang, "Study on injection molding process simulation and process parameter optimization of automobile instrument light guiding support," *Advances in Materials Science and Engineering*, vol. 2021, Article ID 9938094, pp. 2021–2113, 2021.

[21] O. A. Adefuye, O. Ji, L. Oi, and O. Fadipe, "Gating System Design Solutions for Casting Defects from Pouring," *Engineering and Technology Research Journal*, vol. 5, no. 1, 2020.

[22] Y. Yang and M. Wang, "Using MOLDFLOW to optimize the gating system of bucket injection mould[C]//IOP conference series: materials science and engineering," *IOP Conference Series: Materials Science and Engineering*, vol. 394, no. 3, Article ID 032065, 2018.

[23] J. Feng, X. Tang, and W. Wang, "Reliability verification method of numerical simulation based on grid independence and time independence," *Journal of Shihezi University*, vol. 35, no. 01, pp. 52–56, 2017.

[24] M. Kugler, A. Hostettler, L. Soler, Y. Remond, and D. George, "A new algorithm for volume mesh refinement on merging

geometries: a," *Journal of Computational and Applied Mathematics*, vol. 330, pp. 429–440, 2018.

[25] W. QingZhao, *Study on Optimization and Vibration Reduction of Plastic Centrifugal Pump Transmission system*, Anhui Polytechnic University, Wuhu, China, 2021.

[26] C. T. Pan, Y. M. Hwang, Y. M. Lin et al., "Development of p microspheres with controllable and uniform particle size by uniform design experiment in emulsion progress," *Sensors and Materials*, vol. 31, no. 2, pp. 311–318, 2019.

[27] Q. Zhiwen, L. Junhui, and Z. Tianwenet, "Process optimization analysis of warpage in injection molding of thin wall plastic parts," *Electromechanical Engineering Technology*, vol. 51, no. 02, pp. 170–172+188, 2022.

[28] B. Shiroud Heidari, A. Hedayati Moghaddam, S. M. Davachi, S. Khamani, and A. Alihosseini, "Optimization of process parameters in plastic injection molding for minimizing the volumetric shrinkage and warpage using radial basis function (RBF) coupled with the k-fold cross validation technique," *Journal of Polymer Engineering*, vol. 39, no. 5, pp. 481–492, 2019.

[29] J. I. Daoud, "Multicollinearity and regression analysis[C]// Journal of physics: conference series," *Journal of Physics: Conference Series*, vol. 949, no. 1, Article ID 012009, 2017.

[30] L. Li, F. Liu, B. Chen, and C. B. Li, "Multi-objective optimization of cutting parameters in sculptured parts machining based on neural network," *Journal of Intelligent Manufacturing*, vol. 26, no. 5, pp. 891–898, 2015.

[31] O. Kramer, "Genetic algorithms," *Genetic Algorithm Essentials*, pp. 11–19, Springer Cham, Midtown Manhattan, New York, 2017.